Research Square

Preprints are preliminary reports that have not undergone peer review.
They should not be considered conclusive, used to inform clinical practice,
or referenced by the media as validated information.

Two new species of Trichoderma from agricultural soils in China

Ke-Lin Li
Zhejiang University
Li-Juan Mao
Zhejiang University
Chu-Long Zhang
clzhang@zju.edu.cn

Zhejiang University https://orcid.org/0000-0001-5180-0348

Research Article

Keywords: Hypocreales, Trichoderma, phylogenetic analysis, pairwise sequence similarity, taxonomy

Posted Date: August 6th, 2026

DOI: https://doi.org/10.21203/rs.3.rs-10351503/v1

License: This work is licensed under a Creative Commons Attribution 4.0 International License. Read Full License

Abstract

Trichoderma constitutes a species-rich, globally widespread fungal genus with important agricultural application potential. Multilocus phylogenetic analyses and pairwise nucleotide similarity assessments are performed on isolates representing two putative novel taxa recovered from agricultural soils sampled across multiple Chinese provinces. Phylogenetic reconstructions based on concatenated *rpb2* and *tef1* barcode datasets reveal that all isolates of each candidate taxon form well-resolved, independent monophyletic lineages clearly segregated from every formally published species: *Trichoderma yunguichuanense* falls within Clade 1 (*Harzianum* Clade), and *T. paramoravicum* belongs to Clade 2 (*Moravicum* / *Semiorbis* Clade). Pairwise nucleotide comparisons between the collected isolates and their phylogenetically adjacent reference strains yield similarity values below the dual conspecific cutoffs of ≥ 99% for *rpb2* and ≥ 97% for *tef1*, the molecular thresholds specified in *Trichoderma* barcode guidelines. Meanwhile, multilocus phylogeny and pairwise similarity data demonstrate that *T. longibrachiatum*, *T. awajun*, and *T. bissettii* simultaneously reach the conspecific identity benchmarks, which confirms the three taxa constitute a single conspecific complex. Detailed descriptions of colony features on four standardized culture media and microscopic morphological structures are provided. This taxonomic study enriches the documented diversity of *Trichoderma* resources distributed across Chinese agricultural ecosystems.

Introduction

Trichoderma (*Ascomycota*, *Sordariomycetes*, *Hypocreales*, *Hypocreaceae*) attracts broad mycological research attention owing to its ecological importance and broad application prospects in sustainable agricultural systems (Woo et al. 2023). Multiple taxa within this genus exhibit prominent beneficial biological traits: *Trichoderma harzianum* strain NJAU4742 was confirmed to alleviate maize fusariosis by degrading fusaric acid (Cao et al. 2025); T. *asperellum* FJ035 was verified to reduce successive cropping-associated cucumber fusarium wilt via restructuring rhizosphere microbial assemblages (Zhang et al. 2025); T. *nigricans* T32781 maintains balanced plant-soil interactions and supports sustainable crop production on cadmium-contaminated farmlands (Zhang et al. 2026).

Trichoderma constitutes a species-rich, globally widespread fungal genus. As of 19 June 2026, a total of 533 validly published *Trichoderma* species are documented in Fungal Names (https://nmdc.cn/fungalnames/). Marked interspecific differentiation exists within *Trichoderma*, and accurate species identification acts as a fundamental prerequisite for exploring its functional exploitation. Taxonomic studies on this genus have undergone a key shift from morphology-only identification to phylogeny-driven classification. Cai & Druzhinina (2021) proposed standardized molecular identification criteria based on three DNA barcodes (ITS, *tef1*, and *rpb2*): strains with ≥ 76% ITS sequence identity are classified into the genus *Trichoderma*; isolates carrying ≥ 99% *rpb2* and ≥ 97% *tef1* pairwise similarity are treated as conspecific populations.

Nationwide large-scale surveys of *Trichoderma* resource have been conducted over the past decades, yielding numerous formally described novel lineages, and 211 *Trichoderma* species had been recorded across China by 2020 (Zhuang 2020). Nevertheless, a wide range of habitats remain undersampled, and abundant cryptic *Trichoderma* lineages still await formal taxonomic description. Our research team has discovered more than ten undescribed *Trichoderma* taxa isolated from Chinese agricultural soils and wild *Poaceae*. The present work extends our prior taxonomic research (Zhao et al. 2023; Zhao et al. 2025); multilocus phylogenetic inference, pairwise nucleotide similarity evaluation, and morphological observation were conducted on candidate novel isolates recovered from typical agricultural soils to expand the catalogue of indigenous fungal resources in China.

Materials and methods

Strain isolation and preservation

Trichoderma isolates were recovered from agricultural soil matrices sampled across Guizhou, Sichuan, Yunnan, Jiangsu and Zhejiang Provinces using selective fungal culture media, following previously documented experimental pipelines (Jiang et al. 2016; Dou et al. 2019). All axenic pure cultures are maintained under dual storage conditions at the Institute of Biotechnology, College of Agriculture and Biotechnology, Zhejiang University, Hangzhou, China: short-term preservation at 4°C and long-term cryopreservation at − 80°C ultra-low-temperature freezers. Holotype and ex-type living cultures of the two novel taxa described herein have been deposited at the Guangdong Microbial Culture Collection Center (GDMCC) for permanent metabolically inactive preservation.

Morphological characterization

Morphological observations were performed following standardized taxonomic protocols documented in previous studies (Zhao et al. 2023; Zhao et al. 2025). Four standard culture substrates were adopted for phenotypic characterization: Potato Dextrose Agar (PDA), Cornmeal Dextrose Agar (CMD), Malt Extract Agar (MEA), and Synthetic Nutrient Agar (SNA). Inoculated Petri dishes were incubated at 25°C under a 12 h light / 12 h dark photoperiod for 7 d to record complete colonial traits. Growth gradient experiments were carried out under constant darkness at three temperature gradients (25°C, 30°C, 35°C); colony radial diameters were measured on a daily basis.

Temporary microscopic slides were mounted with lactic acid glycerol as the mounting medium. Morphological structures including conidiophores, phialides, conidia and chlamydospores were observed and photographed under a Nikon Eclipse 80i compound light microscope. A minimum of 30 replicates of phialides and conidia were measured to obtain quantitative morphometric data. All dimensional measurements follow the universal taxonomic format (a–)b–c(–d), where a represents the minimum extreme value, d denotes the maximum extreme value, and the range b–c covers measurements of 90% of all examined individuals.

DNA extraction, PCR amplification, and sequencing

Genomic DNA extraction, PCR amplification and bidirectional Sanger sequencing were conducted using established laboratory workflows (Jiang et al. 2016; Zhao et al. 2023; Zhao et al. 2025). Three pairs of universal fungal primers were used to amplify target barcode fragments: ITS-1/ITS-4 for the ITS region (White et al. 1990), EF1/EF2 for *tef1* (O'Donnell et al. 1998), and fRPB2-5F/fRPB2-7cR for *rpb2* (Liu et al. 1999). Identical forward and reverse primer sets were applied for bidirectional sequencing. All novel nucleotide sequences generated in the present study have been submitted and archived in the NCBI GenBank public database.

Multilocus phylogenetic analyses and sequence similarity calculation

All phylogenetic workflows were executed on the PhyloSuite platform (Xiang et al. 2023). Reference barcode sequences of validly published *Trichoderma* species were retrieved from the GenBank repositories. A total of 182 taxa were incorporated into the final concatenated dataset, with *Protocrea farinosa* C.P.K. 3144 and *P. pallida* CBS 299.78 designated as outgroup taxa for tree rooting. Full GenBank accession information for all analysed strains are provided in Table 1.

Table 1
GenBank accession numbers of ITS, *rpb*2, and *tef*1 sequences for *Trichoderma* taxa used in this study. Novel sequences generated in this study are highlighted in bold font.

Clade	Current species	Specimen/Culture number	ITS	*rpb2*	*tef1*	Genome
outgroup	*Protocrea farinosa*	C.P.K. 3144	EU703917	EU703938	EU703894	
outgroup	*P. pallida*	CBS 299.78 (T)	NR_111329	EU703948	EU703900	
1	*Trichoderma afroharzianum*	CBS 124620, G.J.S. 04-186 (ET)	NR_137304	FJ442691	FJ463301	
1	*T. afroharzianum*	G.J.S. 04-193	FJ442233	FJ442709	FJ463298	
1	*T. afroharzianum*	G.J.S. 04-197	FJ442214	FJ442740	FJ463302	
1	*T. afroharzianum*	HZA3	MH624138	MH647793	MK850825	
1	*T. afroharzianum*	T22	–	KP009145	KP008850	JGI 1185335
1	*T. afroharzianum*	T6776	GU997086	genome	genome	GCA_000988865.1
1	*T. afroharzianum*	TRS835	KP009351	KP009149	KP008787	
1	*T. aggregatum*	HMAS 248863, CGMCC 3.18406 (T)	NR_154582	KY688001	KY688062	
1	*T. aggregatum*	HMAS 248864	KY687947	KY688002	KY688063	
1	*T. aggressivum*	CBS 100525	–	AF545541	AF348095	
1	*T. aggressivum*	CBS 100526	FJ442607	KP009166/ genome	KP008993/ genome	GCA_033847375.1
1	*T. aggressivum*	DAOM 222156 (ET)	NR137299	FJ442752	AF348098	
1	*T. albidum*	YMF 1.7530 (T)	OQ517962	OQ559127	OQ559118	
1	*T. albidum*	YMF 1.7531	OQ517963	OQ559128	OQ559119	
1	*T. alni*	C.P.K. 2494	EU518652	EU498350	EU498313	
1	*T. alni*	CBS 120633, C.P.K. 1982, Hypo 254 (T)	NR_134375	EU498349	EU498312	
1	*T. alpinum*	HMAS 248821, CGMCC 3.18385 (T)	NR_154561	KY687958	KY688012	
1	*T. alpinum*	HMAS 248870	KY687953	KY687963	KY688017	
1	*T. amazonicum*	CBS 126898, IB 50 (T)	HM142358	HM142367	HM142376	
1	*T. amazonicum*	IB 95	HM142359	HM142368	HM142377	
1	*T. asiaticum*	YMF 1.00168	MH262582	MH262575	MH236492	
1	*T. asiaticum*	YMF 1.00352 (T)	MH113930	MH158994	MH183183	
1	*T. atrobrunneum*	G.J.S. 04–67	FJ442273	FJ442724	FJ463360	
1	*T. atrobrunneum*	CBS 548.92, G.J.S. 92–110 (T)	NR_137298	–	AF443942	
1	*T. atrobrunneum*	T42	KX632515	KX632572	KX632629	
1	*T. atrogelatinosum*	CBS 237.63 (T)	AF400751	KJ842201	–	
1	*T. atrogelatinosum*	DAOM 167632	–	–	KJ871083	
1	*T. atrogelatinosum*	LU498	–	KJ842176	KJ871087	
1	*T. azadirachtae*	ZHKUCC 24–0201 (T)	PP551629	PP556389	PP556386	
1	*T. azadirachtae*	ZHKUCC 24–0202 (T)	PP551630	PP556390	PP556387	
1	*T. azadirachtae*	ZHKUCC 24–0203 (T)	PP551631	PP556391	PP556388	
1	*T. azevedoi*	CEN1422 (T)	MK714902	MK696821	MK696660	
1	*T. azevedoi*	CEN1423	MK714903	MK696822	MK696661	
1	*T. bannaense*	HMAS 248840, CGMCC 3.18394 (T)	NR_154570	KY687979	KY688037	
1	*T. bannaense*	HMAS 248865	KY687948	KY688003	KY688038	

Clade	Current species	Specimen/Culture number	ITS	*rpb2*	*tef1*	Genome
1	*T. breve*	HMAS 248844, CGMCC 3.18398 (T)	NR_154574	KY687983	KY688045	
1	*T. breve*	HMAS 248845	KY687928	KY687984	KY688046	
1	*T. brunneoviride*	CBS 120928	EU518661	EU498358	EU498318	
1	*T. brunneoviride*	CBS 121130, Hypo 170 (T)	NR_134376	EU498357	EU498316	
1	*T. camerunense*	G.J.S. 99–230 (T)	NR_137300	genome	AF348107	GCA_050948025.1
1	*T. camerunense*	G.J.S. 99–231	AY027783	–	AF348108	
1	*T. catoptron*	CBS 114232, DAOM 232830, G.J.S. 02–76 (T)	NR_134348	AY391900	AY737726	
1	*T. cavernicola*	GMBCC1103 (T)	PQ654705	PV067157	PV132334	
1	*T. cavernicola*	GMBCC1105	PQ654706	PV067158	PV132335	
1	*T. ceraceum*	CBS 114245, DAOM 232831, G.J.S. 95–159 (T)	EU330953	AF545508	AY937437	
1	*T. cerinum*	CBS 136992, S357	–	KF134788	KF134797	
1	*T. cerinum*	DAOM 230012, ATCC MYA-4840 (ET)	NR_111835	KJ842184	AY937443	
1	*T. cinnamomeum*	CBS 114235, DAOM 232833, G.J.S. 97–230 (T)	–	AY391918	–	
1	*T. cinnamomeum*	G.J.S. 97–233	–	AY391919	–	
1	*T. cinnamomeum*	G.J.S. 97–237	NR_144871	AY391920	AY737732	
1	*T. confertum*	HMAS 248893	–	MF371203	MF371218	
1	*T. confertum*	HMAS 248896 (T)	–	MF371205	MF371220	
1	*T. crassum*	CBS 336.93	MH862406	–	AF401021	
1	*T. crassum*	KUC21313	–	MZ302964	MZ302977	
1	*T. crassum*	TRS113	KP009300	KP009102	KP008865	
1	*T. crassum*	DAOM 164916 (T)	NR_134370	AF545542	EU280048 + AF534615	
1	*T. densissimum*	T31818	–	OP357965	OP357967	
1	*T. densissimum*	T32353	–	OP357964	OP357970	
1	*T. densissimum*	T32434 (T)	–	OP357966	OP357971	
1	*T. densissimum*	T32465	–	OP357963	OP357972	
1	*T. graminicola*	YNE00489	–	OR779493	OR779520	
1	*T. graminicola*	YNE00490 (T)	–	OR779494	OR779521	
1	*T. guizhouense*	CBS 131803 (T)	JN191311	JQ901400	JN215484	
1	*T. guizhouense*	HGUP0039	JX089584	JQ901401	JX089585	
1	*T. harzianum*	CBS 226.95 (NT)	AY605713	AF545549	AF348101	GCA_003025095.1
1	*T. harzianum*	TRS55	KP009211	KP009121	KP008803	
1	*T. harzianum*	TRS94	KP009250	KP009120	KP008802	
1	*T. hausknechtii*	CBS 133493 (T)	–	KJ665276	KJ665515	
1	*T. helicolixii*	CBS 133499 (T)	–	KJ665278	KJ665517	GCA_001990665.1
1	*T. helicolixii*	CBS 135583	–	KJ665277	KJ665516	
1	*T. hirsutum*	HMAS 248834 (T)	NR_154565	KY687972	KY688029	
1	*T. hirsutum*	HMAS 248859	KY687942	KY687998	KY688030	
1	*T. jilotepecense*	IE 7000 (T)	PV687646	PV694671	PV694678	
1	*T. jilotepecense*	IE 7001	PV687647	PV694672	PV694679	
1	*T. jilotepecense*	IE 7002	PV687648	PV694673	PV694680	

Clade	Current species	Specimen/Culture number	ITS	*rpb2*	*tef1*	Genome
1	*T. koreanum*	SFC 20131005-S066 (T)	MH050352	MH025988	MH025979	
1	*T. koreanum*	SFC20130926-S004	–	MH025990	MH025982	
1	*T. linzhiense*	HMAS 248846 (T)	NR_154575	KY687985	KY688047	
1	*T. linzhiense*	HMAS 248874	KY687957	KY688011	KY688048	
1	*T. neocrassum*	CBS 114230, G.J.S. 01-227 (T)	–	AY481587	JN133572	
1	*T. parapeberdyi*	T30677 (T)	–	OR779483	OR779510	
1	*T. parapeberdyi*	T32471	–	OR779484	OR779511	
1	*T. peberdyi*	CEN1387	MK714861	MK696781	MK696619	
1	*T. peberdyi*	CEN1426 (T)	MK714906	MK696825	MK696664	
1	*T. perfasciculatum*	YMF 1.07894 (T)	PP213139	PP388992	PP405577	
1	*T. perfasciculatum*	YMF 1.08103	PP213138	PP388991	PP405576	
1	*T. pinicola*	KACC 48486 (T)	NR_173781	MH025993	MH025981	
1	*T. pinicola*	SFC20130926-S014	–	MH025991	MH025978	
1	*T. polypori*	HMAS 248855 (T)	NR_154580	KY687994	KY688058	
1	*T. polypori*	HMAS 248861	KY687944	KY688000	KY688059	
1	*T. pseudogelatinosum*	CNUN309	HM769754	HM920173	HM920202	
1	*T. pseudogelatinosum*	TUFC 60186 (T)	NR_144878	JQ797405	JQ797397	
1	*T. pseudogelatinosum*	TUFC 60933	JQ797391	JQ797407	JQ797399	
1	*T. robustum*	YMF 1.08101 (T)	PP213136	PP388988	PP405573	
1	*T. simplex*	HMAS 248842 (T)	NR_154572	KY687981	KY688041	
1	*T. simplex*	HMAS 248860	KY687943	KY687999	KY688042	
1	*T. tomentosum*	DAOM 1787 13a (T)	NR_134357	AF545557	AY750882	
1	*T. tomentosum*	S33	–	KF134793	KF134801	
1	*T. tomentosum*	GZDS1101	OL831018	OL869951	OL869948	
1	*T. tomentosum*	S23	–	KJ665351	KJ665759	
1	*T. velutinum*	DAOM 230013 (ET)	AF149873	JN133569	KJ665769	
1	*T. velutinum*	LESF132	KT278865	KT278954	KT279019	
1	*T. virens*	DAOM 167652	EU330955	AF545547	AY750891	
1	*T. virens*	DIS 162	FJ442669	FJ442696	FJ463367	
1	*T. virens*	Gv29-8	–	genome	genome	GCA_000170995.2
1	*T. virens*	HZA14	MH624149	MH647804	MK850836	
1	*T. viridulum*	HMAS 273865 (T)	–	KX026965	KX026957	
1	*T. viridulum*	HMAS 273866	–	KX026964	KX026956	
1	*T. yilanense*	BCRC 18F0052 (T)	PP786515	PP779116	PP779115	
1	*T. yunguichuanense*	T33275	PZ535900	PZ530639	PZ540330	
1	*T. yunguichuanense*	T33343	PZ535904	PZ530643	PZ540331	
2	*T. changbaiense*	HMAS 247198 (T)	–	MF371209	MF371224	
2	*T. fertile*	DAOM 167161 (T)	NR_134336	AF545546	KJ871131	
2	*T. fomiticola*	CBS 121136 (T)	NR_134391	FJ860538	FJ860639	
2	*T. hunua*	CBS 238.63 (T)	NR_160091	KJ665279	KJ665519	
2	*T. mienum*	CBS 132690, TUFC 61533 (T)	NR_134433	AB856754	AB856681	
2	*T. mienum*	TUFC 61534	JQ621970	JQ621969	JQ621979	
2	*T. moravicum*	C.P.K. 2489	FJ860783	FJ860549	–	

Clade	Current species	Specimen/Culture number	ITS	*rpb2*	*tef1*	Genome
2	*T. moravicum*	CBS 120539, C.P.K. 2418 (ET)	NR_134398	–	FJ860651	
2	*T. fassatiovae*	CCF 5000 (T)	LN866275	LN866276	LN866277	
2	*T. oblongisporum*	DAOM 176226 (T)	–	KJ842199	KJ871142	
2	*T. oblongisporum*	DAOM 167085	NR_138437	AF545551	AY750884	
2	*T. paramoravicum*	T30466	PZ535901	PZ530640	PZ540332	
2	*T. paramoravicum*	T31062	PZ535902	PZ530641	PZ540334	
2	*T. paramoravicum*	T33135	PZ535903	PZ530642	PZ540333	
2	*T. semiorbis*	DAOM 167636	AY737758	AF545522	KJ871120 + AY737750	
2	*T. semiorbis*	G.J.S. 99–108 (T)	NR_134423	JN133567	JN133576	
3	*T. aethiopicum*	CBS 130628, G.J.S. 10–166, C.P.K. 1837 (T)	MH865819	HM182986/ genome	EU401615/ genome	GCA_051819885.1
3	*T. aethiopicum*	CBS 130627, C.P.K.1817, G.J.S. 10–165	MH865820	–	EU401614	
3	*T. aquaticum*	YMF 1.04624	MH383057	MK775511	MK775506	
3	*T. aquaticum*	YMF 1.04625 (T)	MH383058	MK775512	MK775507	
3	*T. longibrachiatum* (= *awajun*)	CP24-7 (T)	–	MW480147	MW480138	
3	*T. longibrachiatum* (= *awajun*)	CP24-8	–	MW480148	MW480139	
3	*T. beinartii*	OY 7107	FJ571493	–	FJ619252	
3	*T. beinartii*	PPRI 19281 (T)	NR_159032	–	KX267782	
3	*T. caeruleimontis*	PPRI 23903 (T)	KX267813	–	KX267792	
3	*T. centrosinicum*	HMAS 248756	–	KX066268	KX066258	
3	*T. centrosinicum*	HMAS 248755 (T)	–	KX066267	KX066257	
3	*T. flavescens*	HMJAU 34654	–	KX765304	KX765305	
3	*T. flavescens*	HMJAU 34730 (T)	–	KU235486	KU235485	
3	*T. ghanense*	G.J.S. 95–137, IAM 13109, ATCC 208858 (T)	NR_120299	JN175559	AY937423	
3	*T. ghanense*	CCMA-1212	–	genome	genome	GCA_004382785.1
3	*T. gracile*	G.J.S. 10–263 (T)	–	JN175547	JN175598	GCA_051819905.1
3	*T. indicum*	NFCCI 5214 (T)	–	ON952501	ON951920	
3	*T. indicum*	NFCCI 5549	–	OR192143	OR192144	
3	*T. kunigamense*	TAMA 193 (T)	NR_134334	AB807657	AB807645	
3	*T. littericola*	URMicro 11723 (T)	–	OR762231	OR762227	
3	*T. longibrachiatum* (= *bissettii*)	CBS 137447, UTHSC 08-2443, FMR 12635 (T)	KJ174235	–	HG931266	
3	*T. longibrachiatum* (= *bissettii*)	SZMC 25718	MN329160	MN650681	MN641029	
3	*T. longibrachiatum*	CBS 816.68, ATCC 18648 (T)	NR_120298	HQ260615	AY865640 + AY937412	GCA_003025155.1
3	*T. longibrachiatum*	DAOM 166989	EU330961	EU338339	EU338335	
3	*T. longibrachiatum*	T30080	PZ535898	PZ530638	PZ540327	
3	*T. longibrachiatum*	T30195	PZ535897	PZ530637	PZ540326	
3	*T. longibrachiatum*	T30406	PZ535908	PZ530644	PZ540328	
3	*T. longibrachiatum*	T32817	PZ535909	PZ530645	PZ540329	
3	*T. orientale*	CBS 131488	JQ685873	JQ685884	JQ685868	

Clade	Current species	Specimen/Culture number	ITS	*rpb2*	*tef1*	Genome
3	*T. orientale*	CBS 130428, G.J.S. 88 – 81 (T)	NR_111317	–	EU401581	
3	*T. orientale*	GJS 09-784	–	JN175522	JN175578	
3	*T. parareesei*	CBS 125925 (T)	–	HM182963/ genome	GQ354353, genome	GCA_001050175.1
3	*T. parareesei*	CP10-3	–	MW541108	MW541128	
3	*T. pinnatum*	G.J.S. 02-120	–	JN175516	JN175572	
3	*T. pinnatum*	G.J.S. 04-100 (T)	–	JN175515	JN175571	
3	*T. pluripenicillatum*	YMF 1.06198 (T)	MN977788	MT070160	MT070159	
3	*T. reesei*	CBS 999.97	–	genome	genome	GCA_001999515.1
3	*T. reesei*	QM6a (T)	Z31016	HM182969	Z23012	GCA_002006585.1
3	*T. rugosum*	HMAS 247269 (T)	–	MH612373	MH612379	
3	*T. rugosum*	HMAS 247270	–	MH612372	MH612378	
3	*T. thermophilum*	HMAS 248757	–	KX066262	KX066250	
3	*T. thermophilum*	HMAS 252912 (T)	–	KX066261	KX066249	
3	*T. tsugarense*	TAMA203 (T)	NR_134335	AB807659	AB807647	
3	*T. xanthum*	HMAS 247207 (T)	–	MF371211	MF371226	
5	*T. koningii*	ATCC 64262	NR_138456	–	AY376046	
5	*T. koningii*	CBS 119500	FJ860762	FJ860541	KC285594	
5	*T. koningii*	CBS 457.96 (NT)	MH862585	–	AF456909	
5	*T. koningii*	G.J.S. 89–122 (T)	AY380902	–	AY376045	
5	*T. koningii*	G.J.S. 90 – 18	DQ323409	EU248600	DQ289007	
5	*T. viride*	CBS 101526	AY380908	EU248599	AY376053	
5	*T. viride*	CBS 119325 (ET)	NR_138441	EU711362	DQ672615	
5	*T. viride*	CBS 119327	DQ677657	–	DQ672617	
5	*T. viride*	TRS575	KP009372	KP009081	KP008931	

Raw single-locus sequences were aligned with MAFFT v7.505 (Katoh & Standley 2013). Ambiguous flanking regions were manually trimmed in MEGA7 to match the standardized barcode fragment lengths specified for genus-wide *Trichoderma* species identification (Cai & Druzhinina 2021). Terminal gaps were coded as missing data (denoted by "?") before individual single-gene matrices were concatenated into a combined *rpb2* + *tef1* dataset. Partitioned substitution models were selected via ModelFinder v2.2.0 (Kalyaanamoorthy et al. 2017) based on the Bayesian Information Criterion (BIC), with edge-linked proportional rate variation enabled.

Maximum Likelihood (ML) phylogeny was inferred in IQ-TREE v2.2.0 under the optimal partition-specific substitution models: TNe + I+G4 for the *rpb2* partition and TN + F+I+R3 for the *tef1* partition. Nodal support was evaluated with three metrics: 10,000 ultrafast bootstrap (UFBoot) replicates, the SH-like approximate likelihood ratio test (SH-aLRT), and the aBayes test. Partition-specific relative evolutionary rates were estimated to account for rate heterogeneity across the two gene loci.

Bayesian Inference (BI) was implemented in MrBayes 3.2.6 using the best-fit models: K2P + I+G4 for *rpb2* and HKY + F+I+G4 for *tef1*. Two independent Markov chain Monte Carlo (MCMC) runs were operated for 1,000,000 generations with sampling every 2000 generations. The initial 25% of sampled trees were discarded as burn-in to eliminate pre-convergence artefacts. Three standard convergence diagnostics were applied to validate MCMC stationarity: average standard deviation of split frequencies (ASDSF), potential scale reduction factor (PSRF), and effective sample size (ESS). Convergence was deemed reliable when ESS > 100 and PSRF approximated 1.0.

The resulting ML and BI phylogenetic trees were visualized, labelled and annotated via the TVBOT online tool (https://www.chiplot.online/tvbot.html; (Xie et al. 2023), followed by post-processing and layout refinement in Adobe Illustrator v.27.0. Nodal support values are only displayed on branches where ultrafast ML bootstrap (MLBS) ≥ 70 and Bayesian posterior probability (BPP) ≥ 0.9.

Pairwise nucleotide identity calculations and molecular species delimitation thresholds strictly followed the criteria established by Cai & Druzhinina (2021). All pairwise sequence comparisons between newly obtained isolates and their closely related *Trichoderma* relatives were computed via ClustalOMEGA (https://www.ebi.ac.uk/Tools/msa/clustalo/). Isolates sharing ≥ 76% ITS similarity with reference sequences were assigned to the genus *Trichoderma*. Isolates satisfying both cutoffs (≥ 99% identity for *rpb2*, ≥ 97% identity for *tef1*) were recognised as conspecific, whereas lineages failing to meet these dual similarity thresholds were regarded as phylogenetically distinct, undescribed species with robust molecular support.

Results

Sequence analyses

The concatenated *rpb2* + *tef1* alignment comprised 182 taxa spanning 1,506 aligned nucleotide positions, including 682 parsimony-informative sites, 60 singleton sites, and 764 constant sites, with a low missing data fraction of 0.055.

ML analysis yielded an optimal log-likelihood score of − 20290.351 and a total tree length of 4.330. Marked heterogeneity in evolutionary rate was detected between the two gene partitions under the edge-linked proportional model: partition-specific relative substitution rates were estimated at 0.518 for *rpb2* and 1.565 for *tef1*. This result indicated that *tef1* evolves approximately three times faster than *rpb2*. Such rate disparity conferred complementary phylogenetic resolution: the relatively conserved *rpb2* provided a stable backbone for higher-level infrageneric delineation, whereas rapidly variable sites within *tef1* resolved closely related congeneric species. Nodal support across the phylogeny was uniformly strong, with most internal branches receiving UFBoot ≥ 95%, SH-aLRT ≥ 80%, and aBayes ≥ 0.95, confirming the robustness of inferred evolutionary relationships.

All Bayesian MCMC chains converged satisfactorily with stable parameter estimates. The final ASDSF value reached 0.010058, well below the standard convergence cutoff of 0.06. All PSRF values approximated 1.0, and the ESS values exceeded 220, far surpassing the empirical threshold of 100; these metrics verified adequate posterior sampling and reliable parameter optimisation. The harmonic mean likelihood across the two independent BI runs totalled − 20755.29. Consistent evolutionary parameters were recovered for each partition, with a mean total tree length of 3.837, average transition–transversion ratio (kappa) of 4.337, and mean proportion of invariable sites (pinvar) of 0.453.

Topologies generated by ML and BI were highly congruent, with no topological conflicts observed among major well-supported clades. Most internal branches received robust support across three ML metrices (UFBoot, SH-aLRT, aBayes) and high BPP, demonstrating that combined *rpb2* and *tef1* barcodes provide powerful discriminatory resolution for interspecific relationships within *Trichoderma*. All ingroup isolates and reference strains clustered into four distinct, strongly supported major clades (Clade 1, 2, 3, and 5, Fig. 1), consistent with the genus-wide phylogenetic framework outlined by Cai & Druzhinina (2021).

Clade 1 (the *Harzianum* Clade) accommodates representative taxa including *T. aggressivum*, *T. harzianum* and *T. virens*. Strains T33275 and T33343 formed an independent, fully supported monophyletic subclade (100% MLBS / 1.00 BPP) nested within a larger robust lineage containing closely allied species: *T. ceraceum*, *T. cerinum*, *T. koreanum*, *T. linzhiense*, *T. parapeberdyi*, *T. peberdyi*, *T. tomentosum*, *T. viridulum*. Pairwise similarity calculations against all close relatives (Table 2) demonstrated that neither isolate satisfied the dual conspecific similarity thresholds (≥ 99% for *rpb2*, ≥ 97% for *tef1*). In line with the barcode criteria—distinct monophyletic lineages failing to meet both conspecific similarity cutoffs are recognised as valid novel species—these two strains were formally confirmed as a single undescribed taxon.

Pairwise *rpb2* and *tef1* sequence similarity (%) between *T*

Strain	*T.ceraceum* CBS 114245 T	*T.cerinum* CBS 136992	*T.cerinum* DAOM 230012 ET	*T.koreanum* SFC20130926-S004	*T.koreanum* SFC20131005-S066 H	*T.linzhiense* HMAS 248846 H	*T.linzhiense* HMAS 248874	*T.parape* T30677
T.ceraceum CBS 114245 T	**100.00**/100.00	**97.66**/90.46	97.49/90.02	**97.42**/86.43	**97.29**/86.43	**97.79**/91.39	**97.79**/91.39	**98.15/9**
T.cerinum CBS 136992	**97.66**/90.46	**100.00**/100.00	99.47/98.97	**97.79**/93.00	**97.79**/93.00	**99.51**/97.92	**99.51**/97.92	**97.05/9**
T.cerinum DAOM 230012 ET	97.49/90.02	99.47/98.97	100.00/100.00	97.88/90.24	97.88/90.24	99.21/97.29	99.21/97.29	96.96/9
T.koreanum SFC20130926-S004	**97.42**/86.43	**97.79**/93.00	97.88/90.24	**100.00**/100.00	**99.88**/99.13	**97.66**/93.35	**97.66**/93.35	**96.56/8**
T.koreanum SFC20131005-S066 H	**97.29**/86.43	**97.79**/93.00	97.88/90.24	**99.88**/99.13	**100.00**/100.00	**97.66**/93.35	**97.66**/93.35	**96.43/8**
T.linzhiense HMAS 248846 H	**97.79**/91.39	**99.51**/97.92	99.21/97.29	**97.66**/93.35	**97.66**/93.35	**100.00**/100.00	**100.00**/100.00	**97.17/9**
T.linzhiense HMAS 248874	**97.79**/91.39	**99.51**/97.92	99.21/97.29	**97.66**/93.35	**97.66**/93.35	**100.00**/100.00	**100.00**/100.00	**97.17/9**
T.parapeberdyi T30677 T	**98.15**/92.02	**97.05**/93.15	96.96/92.22	**96.56**/87.31	**96.43**/87.31	**97.17**/92.87	**97.17**/92.87	**100.00/**
T.parapeberdyi T32471	**98.03**/92.02	**96.92**/93.15	96.83/92.22	**96.43**/87.31	**96.31**/87.31	**97.05**/92.87	**97.05**/92.87	**99.88/1**
T.peberdyi CEN1387	98.15/89.26	96.96/90.25	96.96/89.34	96.69/84.72	96.56/84.72	97.09/90.11	97.09/90.11	99.74/9
T.peberdyi CEN1426 T	98.15/89.26	96.96/90.25	96.96/89.34	96.69/84.72	96.56/84.72	97.09/90.11	97.09/90.11	99.74/9
T33275	**97.79**/89.46	**97.91**/92.15	98.02/91.45	**97.17**/86.71	**97.17**/86.71	**98.03**/91.65	**98.03**/91.65	**97.17/9**
T33343	**97.91**/89.44	**98.03**/92.13	98.15/91.43	**97.29**/86.68	**97.29**/86.68	**98.15**/91.63	**98.15**/91.63	**97.29/9**
T.tomentosum DAOM 178713a T	**97.17**/91.82	**97.54**/93.98	97.75/93.21	**98.52**/87.96	**98.40**/87.96	**97.42**/93.92	**97.42**/93.92	**96.31/9**
T.tomentosum GZDS1101	**97.42**/91.30	**97.79**/93.26	97.88/92.63	**100.00**/93.27	**99.88**/93.27	**97.66**/93.70	**97.66**/93.70	**96.56/9**
T.tomentosum S23	**97.42**/91.30	**97.79**/93.26	97.88/92.63	**100.00**/93.27	**99.88**/93.27	**97.66**/93.70	**97.66**/93.70	**96.56/9**
T.tomentosum S33	**97.66**/92.02	**98.03**/93.17	98.15/92.55	**99.02**/90.48	**98.89**/90.48	**97.91**/93.50	**97.91**/93.50	**96.80/9**
T.viridulum HMAS 273865 T	**97.29**/90.91	**97.66**/93.92	97.75/93.29	**99.88**/93.53	**99.75**/93.53	**97.54**/94.35	**97.54**/94.35	**96.43/9**
T.viridulum HMAS 273866	**97.29**/90.91	**97.66**/93.92	97.75/93.29	**99.88**/93.53	**99.75**/93.53	**97.54**/94.35	**97.54**/94.35	**96.43/9**

*Bold font indicates that the similarity data originates from a full-length sequence.

Clade 2 (the *Moravicum* = *Semiorbis* Clade) is typified by *T. oblongisporum*. Strains T30466, T31062 and T33135 grouped into a discrete, fully supported monophyletic subclade (100% MLBS / 1.00 BPP) embedded within a well-resolved lineage comprising *T. oblongisporum*, *T. fassatiovae*, and *T. moravicum*. Cross-taxon pairwise similarity comparisons (Table 3) showed consistent divergence below the dual conspecific cutoffs. Following the unified species-delimitation rules for *Trichoderma*, these three isolates represent a second previously unrecognised species-level lineage.

Table 3
Pairwise *rpb2* and *tef1* sequence similarity (%) between *Trichoderma paramoravicum* isolates (T30466, T31062, T33135) and their phylogeneti

Strain	***T.fassatiovae* CCF 5000 T**	***T.fertile* DAOM 167161 T**	***T.mienum* CBS 132690 T**	***T.mienum* TUFC 61534**	***T.moravicum* CPK 2489 / CBS 120539 ET**	***T.oblongisporum* DAOM 167085**	***T.oblongisporum* DAOM 176226 T**	**T30**
T.fassatiovae CCF 5000 T	**100.00**/100.00	**97.05**/87.59	**95.45/85.93**	95.07/68.46	**96.80**/84.07	**98.40/87.62**	98.54/100.00	**97.9**
T.fertile DAOM 167161 T	**97.05**/87.59	**100.00**/100.00	**95.45/87.10**	95.93/66.84	**96.80**/80.00	**96.92/84.60**	96.69/87.59	**97.4**
T.mienum CBS 132690 T	**95.45**/85.93	**95.45**/87.10	**100.00/100.00**	99.14/74.61	**95.20**/81.69	**95.33/83.52**	95.50/86.10	**96.0**
T.mienum TUFC 61534	95.07/68.46	95.93/66.84	99.14/74.61	100.00/100.00	94.86/70.28	95.29/69.21	95.29/68.46	96.1
T.moravicum CPK 2489 / CBS 120539 ET	**96.80**/84.07	**96.80**/80.00	**95.20/81.69**	94.86/70.28	**100.00**/100.00	**96.80/83.16**	96.56/84.24	**97.4**
T.oblongisporum DAOM 167085	**98.40**/87.62	**96.92**/84.60	**95.33/83.52**	95.29/69.21	**96.80**/83.16	**100.00/100.00**	98.15/87.79	**97.7**
T.oblongisporum DAOM 176226 T	98.54/100.00	96.69/87.59	95.50/86.10	95.29/68.46	96.56/84.24	98.15/87.79	100.00/100.00	97.7
T30466	**97.91**/89.04	**97.42**/87.72	**96.06/85.85**	96.15/69.13	**97.42**/84.17	**97.79/90.65**	97.75/89.21	**100**
T31062	**97.91**/89.04	**97.42**/87.72	**96.06/85.85**	96.15/69.13	**97.42**/84.17	**97.79/90.65**	97.75/89.21	**100**
T33135	**97.91**/89.04	**97.42**/87.72	**96.06/85.85**	96.15/69.13	**97.42**/84.17	**97.79/90.65**	97.75/89.21	**100**

*Bold font indicates that the similarity data originates from a full-length sequence.

Clade 3 (the *Longibrachiatum* Clade) contains the section type species *T. longibrachiatum* alongside *T. reesei*. Four field isolates (T30080, T30195, T30406, T32817) constituted a separate fully supported subclade nested within a broad lineage encompassing reference strains of *T. longibrachiatum*, *T. awajun*, and *T. bissettii*. Full pairwise similarity profiling against the three published taxa (Table 4) revealed that all four field isolates simultaneously satisfied both conspecific similarity benchmarks (≥ 99% for *rpb2*, ≥ 97% for *tef1*), despite minor depressed similarity values arising from truncated, incomplete barcode sequences of *T. awajun* and *T. bissettii*. Per the standard barcodeframework, all taxa satisfying both dual similarity thresholds belong to a single conspecific complex. Under the principle of taxonomic priority, *T. awajun* and *T. bissettii* are proposed as heterotypic synonyms of *T. longibrachiatum*, and the four Chinese agricultural isolates are assigned to *T. longibrachiatum*.

Table 4
Pairwise *rpb2* and *tef1* sequence similarity (%) between strains of *T. longibrachiatum* species complex (including *T. longibrachiatum*,

Strain	***T.awajun* CP24-7 T**	***T.awajun* CP24-8**	**T30195**	**T30080**	**T30406**	**T32817**	***T.bissettii* SZMC 25718**	***T.biss* CBS 13744**
T.awajun CP24-7 T	100.00/100.00	100.00/100.00	99.87/98.38	99.87/98.38	99.87/98.38	99.87/98.61	99.56/97.69	-/97.6
T.awajun CP24-8	100.00/100.00	100.00/100.00	99.87/98.38	99.87/98.38	99.87/98.38	99.87/98.61	99.56/97.92	-/97.9
T30195	99.87/98.38	99.87/98.38	**100.00/100.00**	**100.00/100.00**	**100.00/100.00**	**100.00/99.61**	99.81/92.62	**-/97.1**
T30080	99.87/98.38	99.87/98.38	**100.00/100.00**	**100.00/100.00**	**100.00/100.00**	**100.00/99.61**	99.81/92.62	**-/97.1**
T30406	99.87/98.38	99.87/98.38	**100.00/100.00**	**100.00/100.00**	**100.00/100.00**	**100.00/99.61**	99.81/92.62	**-/97.1**
T32817	99.87/98.61	99.87/98.61	**100.00/99.61**	**100.00/99.61**	**100.00/99.61**	**100.00/100.00**	99.81/93.05	**-/97.3**
T.bissettii SZMC 25718	99.56/97.69	99.56/97.92	99.81/92.62	99.81/92.62	99.81/92.62	99.81/93.05	100.00/100.00	-/96.5
T.bissettii CBS 137447 T	-/97.69	-/97.92	**-/97.11**	**-/97.11**	**-/97.11**	**-/97.33**	-/96.57	**-/100**
T.longibrachiatum CBS 816.68 T	99.73/97.69	99.73/97.92	**99.88/97.11**	**99.88/97.11**	**99.88/97.11**	**99.88/97.33**	100.00/96.57	**-/100**
T.longibrachiatum DAOM 166989	99.72/97.69	99.72/97.92	99.87/97.10	99.87/97.10	99.87/97.10	99.87/97.31	100.00/96.77	-/100.

*Bold font indicates that the similarity data originates from a full-length sequence.

Taxonomy

Trichoderma longibrachiatum Rifai, Mycol. Pap. 116: 42 (1969), Fig. 2

Synonyms:

= *Trichoderma bissettii* Sand.-Den. & Guarro, J. Clin. Microbiol. 52(6): 2117 (2014)

= *Trichoderma awajun* M.S. Calderon, D.E. Bustamante & S. Leiva, Mycologia 113: 1059 (2021)

Notes: This species was formally described by (Rifai 1969) and assigned as the type taxon of section *Longibrachiatum* (Bissett 1984). *Trichoderma bissettii* was erected based on clinical isolates using ITS, *tef1*, and *Chi18* loci (Sandoval-Denis et al. 2014), while *T. awajun* was characterised from cacao agricultural ecosystem using *acl1*, *act*, *rpb2*, and *tef1* markers (Bustamante et al. 2021). Multilocus phylogenetic analyses constructed herein cluster the three published taxa (*T. longibrachiatum*, *T. bissettii*, *T. awajun*) alongside four agricultural soil isolates obtained in this study within one fully supported monophyletic clade. The ex-type strain CBS 137447 of *T. bissettii* lacks available *rpb*2 sequences, and the ex-type strain CP24-7 of *T. awajun* possesses only incomplete *rpb*2 and *tef1* barcodes; such truncated partial sequences lead to slight declines in pairwise nucleotide similarity values. When aligned against the full barcode dataset of the *T. longibrachiatum* ex-type strain CBS 816.68, all four field isolates meet the universal conspecific cut-offs for the genus (≥ 99% identity for *rpb2*, ≥ 97% identity for *tef1*). Accordingly, the four soil isolates collected across China are molecularly assigned to *T. longibrachiatum*. Combined evidence from phylogenetic topology and pairwise sequence comparisons supports the conspecific status of *T. longibrachiatum*, *T. bissettii* and *T. awajun*.. Morphological congruence shared by the three taxa comprises well-developed primary conidiophore axes, predominantly solitary phialides, abundant intercalary sporogenous cells and smooth pale green conidia (Bissett 1984; Sandoval-Denis et al. 2014; Bustamante et al. 2021).

Trichoderma paramoravicum C.L. Zhang & K.L. Li, sp. nov., Fig. 3

Fungal Names: FN 573967.

Etymology. The specific epithet *paramoravicum* refers to its close phylogenetic affinity and high morphological resemblance to *Trichoderma moravicum*.

Type. China: Jiangsu Province, Xuzhou City, 34°15'54"N, 117°11'13"E, isolated from vegetable field soil, August 2014, coll. Y. Jiang, living culture T30466 (Holotype GDMCC 3.1374, stored in a metabolically inactive state); ex-type culture GDMCC 3.1374 = T30466.

Description. Asexual morph: Conidiophores erect, sparsely pyramidal; lateral branches alternate or opposite, diverging at right or acute angles, sterile apical appendages absent. Phialides mostly clustered at branch apices, cylindrical-lageniform with moderately broad bases tapering into short necks; a small number of solitary lateral phialides also occur. Phialide dimensions (n = 30): (4.9–)5.2–11.6(–12.0) × (2.0–)2.1–3.3(–3.4) µm, mean = 8.3 × 2.7 µm; length/width (L/W) ratio (1.7–)1.8–4.3(–5.7), mean = 3.0; basal width (1.4–)1.6–2.8(–3.1) µm, mean = 2.4 µm. Conidia pale grey-green, smooth, subglobose to ovoid; dimensions (n = 30): (3.8–)3.8–4.6(–4.6) × (2.9–)3.0–3.2(–3.3) µm, mean = 4.2 × 3.1 µm; L/W ratio (1.2–)1.3–1.4(–1.5), mean = 1.4. Intercalary chlamydospores rare, ca. 9.7 × 9.8 µm. **Sexual morph**: Undetermined.

Culture characteristics. Optimal growth at 25°C; no mycelial growth occurs at 35°C.

PDA: Colony radii 40–45 mm (25°C) and 36–39 mm (30°C) after 72 h, fully covering plates by day 5 and day 6 respectively. Colonies pale blue-grey green with sparse aerial hyphae and granular radial texture; tiny irregular yellow-green sporulating pustules develop.

MEA: Colony radii 34–36 mm (25°C) and 30–33 mm (30°C) after 72 h, fully covering plates by day 6 and day 7 respectively. Colonies pale greyish green with abundant loose radial aerial hyphae and distinct yellow-green sporulation zones.

CMD: Colony radii 43–47 mm (25°C) and 43 to 44 mm (30°C) after 72 h, fully covering plates by day 5 and day 6 respectively. Colonies pale yellow-green with appressed marginal mycelia; small white globose pustules form around inocula and mature yellow-green without obvious concentric bands.

SNA: Colony radii 17–32 mm (25°C) and 17–26 mm (30°C) after 72 h, fully covering plates by day 6 and day 7 respectively. Colonies pale beige-green with sparse radial vegetative hyphae and well-defined yellow-green conidial rings. No diffusible pigments or characteristic volatile odours observed on test media.

Additional specimens examined. China: Jiangsu Province, Xuzhou City, 34°15'54"N 117°11'13"E, vegetable field soil, October 2014, coll. Y. Jiang, T31062. China: Guizhou Province, Guiding City, 26°31'49.7"N, 107°14'11.3"E, maize field soil, October 2015, coll.. Y. Jiang, T33135.

Notes. Multilocus phylogenetic analyses place this novel species within a strongly supported monophyletic subclade together with the closely allied taxa *T. oblongisporum*, *T. fassatiovae*, and *T. moravicum*. It shares pyramidal conidiophores with right/acute-angled lateral branches and an absence of sterile apical extensions with *T. moravicum*, yet stable micromorphometric differences distinguish the two species: phialides of *T. moravicum* extend up to 20 µm with broader widths, and conidial sizes also differ significantly (Jaklitsch 2011). When compared with *T. oblongisporum*, the latter bears elongated sterile terminal extensions, short compact verticillate phialides and narrow ellipsoidal conidia (Bisset 1991), all of which are absent in *T. paramoravicum*.

Trichoderma yunguichuanense C.L. Zhang & K.L. Li, sp. nov., Fig. 4

Fungal Names: FN 573968.

Etymology. The specific epithet *yunguichuanense* derives from Yunnan, Guizhou and Sichuan Provinces, the geographic regions where this fungus was isolated.

Type. China: Guizhou Province, Liupanshui City, 26°23'16"N, 105°01'45"E, maize field soil, June 2016, coll. Y. Jiang, T33275 (Holotype GDMCC 3.1375, stored in a metabolically inactive state); ex-type culture GDMCC 3.1375 = T33275.

Description. Asexual morph: Conidiophores simply dichotomous; lateral branches alternate or irregular opposite, diverging at acute angles from the main axis. Phialides ampulliform, borne in whorls of 2–3 at branch apices. Phialide measurements (n = 30): (3.8–)4.6–9.9(–10.8) × (2.3–)2.4–3.3(–3.4) µm, mean = 7.2 × 2.7 µm; L/W ratio (1.2–)1.5–3.7(–4.1), mean = 2.5; basal width (1.0–)1.2–2.0(–2.2) µm, mean = 1.6 µm. Conidia mist mint-green, ellipsoidal; dimensions (n = 30): (3.5–)3.5–4.1(–4.1) × (2.5–)2.6–2.8(–2.9) µm, mean = 3.8 × 2.7 µm; L/W ratio (1.2–)1.3–1.5(–1.6), mean = 1.4. Rare intercalary chlamydospores present, ca. 7.1 × 7.6 µm. **Sexual morph**: Undetermined.

Culture characteristics. Optimal growth at 30°C; no mycelial growth occurs at 35°C.

PDA: Colony radii 56–57 mm (25°C) and 61–63 mm (30°C) after 72 h, fully covering plates by day 4 under both temperatures. Colonies mustard-yellow, powdery-villous with radial appressed mycelia; distinct white concentric sporulation rings develop from day 3 and mature into dark yellow-green zones with clear demarcation.

MEA: Colony radii 49–56 mm (25°C) and 56–60 mm (30°C) after 72 h, fully covering plates by day 4 under both temperatures. Colonies blue-grey green with loose radial aerial hyphae; pale green sporulation bands surround inocula, with indistinct zonation upon maturation.

CMD: Colony radii 35–37 mm at 25°C after 72 h, fully covered by day 5; fully covering plates within 72 h at 30°C. Colonies mottled yellow-green with irregular appressed radial mycelia, forming alternating yellow- and dark- green concentric sporulation zones.

SNA: Colony radii 32–36 mm (25°C) and 42–52 mm (30°C) after 72 h, fully covering plates by day 5 under both temperatures. Colonies composed of translucent radial vegetative hyphae bearing scattered pale green pustules forming faint concentric rings. No diffusible pigments or distinct volatile odours produced under all incubation conditions.

Additional specimens examined. **China**: Sichuan Province, Suining City, 30°19'22.3"N, 105°25'30.5"E, maize field soil, June 2016, coll. Y. Jiang, T33273. **China**: Guizhou Province, Liupanshui City, 26°23'16"N, 105°01'45"E, maize field soil, June 2016, coll. Y. Jiang, T33343. China: Yunnan Province, Wenshan City, 23°22'19.2"N, 104°14'52.1"E, maize field soil, October 2016, coll. Y. Jiang, T33344, T33456. China: Guizhou Province, Guiding City, 26°31'13.4"N, 107°14'08.2"E, maize field soil, October 2016, coll. Y. Jiang, T33457.

Notes. Multilocus phylogenetic analysis resolves this species within a well-supported subclade of the *Harzianum* Clade, alongside *T. parapeberdyi*, *T. cerinum*, and *T. linzhiense*.

Comparison with *T. parapeberdyi*, both species produce ampulliform phialides and scarce intercalary chlamydospores, yet conidiophore architecture differs drastically. *Trichoderma yunguichuanense* bears simple dichotomous lateral branches diverging at acute-angle from the main axis, whereas *T. parapeberdyi* forms pyramidal conidiophores with perpendicular opposite branches. The phialides of *T. yunguichuanense* are shorter and narrower with thinner bases (mean 7.2 × 2.7 µm, base 1.6 µm), relative to*T. parapeberdyi* (mean 9.4 × 2.9 µm, basal width2.2 µm) (Zhao et al. 2025).

Comparison with *T. cerinum*, both species produce ampulliform phialides and smooth green ellipsoidal conidia. However, *T. cerinum* forms thick, curved primary conidiophore axes with elongated undulate sterile apical extensions (40–90 µm), plus shorter phialides and smaller conidia (2.4–3.5 × 2.0–2.5 µm) (Bissett et al. 2003). In contrast, *T. yunguichuanense* lacks sterile terminal extensions and bears longer phialides as well as larger ellipsoidal conidia.

Comparison with *T. linzhiense*, both species produce green ellipsoidal conidia and chlamydospore. Nevertheless, phialides of *T. linzhiense* are narrowly lageniform and markedly elongated (10.3–15.8 µm) with high L/W ratios ranging from 3.5 to 5.8 (Chen & Zhuang 2017). In contrast, the phialides of *T. yunguichuanense* are shorter ampulliform structures with smaller L/W values (1.5–3.7).

Discussion

Molecular phylogeny has become an essential core tool for modern integrative fungal taxonomy. For species delimitation in the genus *Trichoderma*, Cai & Druzhinina (2021) established objective molecular identification criteria based on the two core barcodes *rpb*2 and *tef1*, together with the unified pairwise sequence similarity thresholds. Phylogenetic analyses based on *rpb2* sequences have resolved eight well-supported infrageneric clades within this genus (Cai & Druzhinina 2021): Clade 1 (*Harzianum* clade) harbours representative species including *T. aggressivum*, *T. harzianum*, and *T. virens*; Clade 2 (*Moravicum / semiorbis* clade) is typified by *T. oblongisporum*; Clade 3 (*Longibrachiatum* clade) accommodates *T. citrinoviride*, *T. longibrachiatum*, and *T. reesei*; Clade 5 (*Viride* clade) includes widely documented taxa such as *T. asperellum*, *T. atroviride*, *T. hamatum*, *T. koningiopsis*, *T. polysporum*, and *T. viride*.

Deficient or incomplete barcode sequences are common among many type strains of published *Trichoderma* species. In such case, integrated analyses of phylogenetic topology and pairwise sequence similarity are required to achieve accurate taxonomic classification. In the present study, concatenated multilocus phylogenetic analyses based on *rpb2* and *tef1* were performed on isolates recovered from agricultural soils across multiple regions of China, along with reference sequences of representative species belonging to Clades 1, 2, 3 and 5. Two phylogenetically distinct lineages were formally described as new species. Among them, *T. yunguichuanense* clustered within Clade 1 (*Harzianum* Clade) and formed an independent monophyletic lineage, while *T. paramoravicum* constituted a separate monophyletic subclade nested in Clade 2 (*Moravicum* Clade). Pairwise sequence similarity comparisons revealed that both new taxa showed similarity values lower than the conspecific cutoffs (≥ 99% for *rpb2*, ≥ 97% for *tef1*) when compared with their closest relatives, which provided robust molecular evidence supporting their status as undescribed species.

Multilocus tree topologies further showed that four soil isolates obtained in this study (T30080, T30195, T30406, T32817) clustered with ex-type and reference strains of three known species, namely *T. longibrachiatum* (CBS 816.68, DAOM 166989), *T. bissettii* (CBS 137447, SZMC 25718) and *T. awajun* (CP24-7, CP24-8), forming a fully supported monophyletic group (100% MLBS, 1.00 BPP). Within this major clade, the four Chinese field isolates constituted an independent subclade with full nodal support; strains of *T. awajun* also formed another fully supported subgroup; whereas strains of *T. longibrachiatum* and *T. bissettii* assembled into a moderately supported subclade without stable interspecific genetic differentiation. Additional pairwise sequence similarity assessment confirmed that the relatively low similarity values between *T. bissettii* and *T. awajun* originated exclusively from their truncated, incomplete barcode sequences. When aligned against the full-length barcode sequences of the *T. longibrachiatum* ex-type strain CBS 816.68, all four indigenous isolates fully met the conspecific similarity thresholds. Combined the topological clustering features and sequence similarity data confirmed that these isolates were conspecific with *T. longibrachiatum*. Accordingly, *T. bissettii* and *T. awajun* are proposed as heterotypic synonyms of *T. longibrachiatum*. This taxonomic treatment is also supported by consistent morphological characteristics shared by the three taxa, including well-developed primary conidiophore axes, mostly solitary terminal phialides, abundant intercalary sporogenous cells and smooth pale green conidia (Bissett 1984; Sandoval-Denis et al. 2014; Bustamante et al. 2021).

Fourteen new *Trichoderma* species have been discovered from agricultural soils and herbaceous *Poaceae* plants in natural habitats across China in our previous taxonomic surveys (Zhao et al. 2023; Zhao et al. 2025). The two novel species reported in the current study were isolated from farmland soils, which further enriches the known species diversity of Chinese *Trichoderma* resources. Continuous fungal resource investigations covering diverse agricultural and natural ecosystems will greatly deepen our understanding of interspecific differentiation, biogeographic distribution patterns and evolutionary trends within the genus *Trichoderma*.

Declarations

Funding

This work was financed by the Provincial Key Research and Development Plan of Zhejiang, China (2020C02027).

Competing Interests

The authors have no relevant financial or non-financial interests to disclose.

Author Contributions

Chu-Long Zhang contributed to the study conception and design. Material preparation, data collection and analysis were performed by Ke-Lin Li, Li-Juan Mao and Chu-Long Zhang. The first draft of the manuscript was written by Ke-Lin Li and all authors commented on previous versions of the manuscript. All authors read and approved the final manuscript.

Data Availability

The sequences generated during the current study are available in the NCBI GenBank repository. The datasets analysed during the current study are available from the corresponding author on reasonable request.

References

1. Bisset J (1991) A revision of the genus *Trichoderma*. III. Section *Pachybasium*. Can J Bot 11(69):2373–2417
2. Bissett J (1984) A revision of the genus *Ttrichoderma*. I. Section *Longibrachiatum* sect. nov. Can J Bot 62(5):924–931
3. Bissett J, Szakacs G, Nolan CA, Druzhinina I, Gradinger C, Kubicek CP (2003) New species of *Trichoderma* from Asia. Can J Bot 81(6):570–586. https://doi.org/10.1139/b03-051
4. Bustamante DE, Calderon MS, Leiva S, Mendoza JE, Arce M, Oliva M (2021) Three new species of *Trichoderma* in the *Harzianum* and *Longibrachiatum* lineages from Peruvian cacao crop soils based on an integrative approach. *Mycologia* 113(5): 1056–1072. https://doi.org/10.1080/00275514.2021.1917243
5. Cai F, Druzhinina IS (2021) In honor of John Bissett: authoritative guidelines on molecular identification of *Trichoderma*. Fungal Divers 107(1):1–69. https://doi.org/10.1007/s13225-020-00464-4
6. Cao L, Shi X, Li T, Zhu H, Liu Y, Pei R, Chen C, Xu Q, Zhang H, Raza W, Logrieco AF, Wang G, Liu D, Shen Q (2025) Fusaric acid detoxification mediates interspecies interactions for sustainable fusarium wilt disease management. Cell Rep 44(11):116531. https://doi.org/10.1016/j.celrep.2025.116531
7. Chen K, Zhuang W (2017) Discovery from a large-scaled survey of *Trichoderma* in soil of China. Sci Rep 7(1):9090. https://doi.org/10.1038/s41598-017-07807-3
8. Dou K, Gao J, Zhang C, Yang H, Jiang X, Li J, Li Y, Wang W, Xian H, Li S, Liu Y, Hu J, Chen J (2019) *Trichoderma* biodiversity in major ecological systems of China. J Microbiol 57(8):668–675. https://doi.org/10.1007/s12275-019-8357-7
9. Jaklitsch WM (2011) European species of *Hypocrea* part II: species with hyaline ascospores. Fungal Divers 48(1):1–250. https://doi.org/10.1007/s13225-011-0088-y
10. Jiang Y, Wang J, Chen J, Mao L, Feng X, Zhang C, Lin F (2016) *Trichoderma* biodiversity of agricultural fields in east China reveals a gradient distribution of species. PLoS ONE 11(8):e160613. https://doi.org/10.1371/journal.pone.0160613

11. Kalyaanamoorthy S, Minh BQ, Wong TKF, von Haeseler A, Jermiin LS (2017) Modelfinder: fast model selection for accurate phylogenetic estimates. Nat Methods 14(6):587–589. https://doi.org/10.1038/nmeth.4285
12. Katoh K, Standley D (2013) Mafft multiple sequence alignment software version 7: improvements in performance and usability. Mol Biol Evol 30:772–780. https://doi.org/10.1093/molbev/mst010
13. Liu YJ, Whelen S, Hall BD (1999) Phylogenetic relationships among ascomycetes: evidence from an RNA polymerse II subunit. Mol Biol Evol 16(12):1799–1808. https://doi.org/10.1093/oxfordjournals.molbev.a026092
14. O'Donnell K, Kistler HC, Cigelnik E, Ploetz RC (1998) Multiple evolutionary origins of the fungus causing Panama disease of banana: concordant evidence from nuclear and mitochondrial gene genealogies. Proc Natl Acad Sci USA 95(5):2044–2049. https://doi.org/10.1073/pnas.95.5.2044
15. Rifai MA (1969) A revision of the genus *Trichoderma*. Mycological Papers 116:1–56
16. Sandoval-Denis M, Sutton DA, Cano-Lira JF, Gené J, Fothergill AW, Wiederhold NP, Guarro J (2014) Phylogeny of the clinically relevant species of the emerging fungus *Trichoderma* and their antifungal susceptibilities. J Clin Microbiol 52(6):2112–2125. https://doi.org/10.1128/JCM.00429-14
17. White TJ, Bruns T, Lee S, Taylor J (1990) Amplification and direct sequencing of fungal ribosomal RNA genes for phylogenetics. In: Innis MA, Gelfand DH, Sninsky JJ, White TJ (eds) PCR Protocols: A Guide to Methods and Applications. Academic Press, Inc., New York, pp 315–322
18. Woo SL, Hermosa R, Lorito M, Monte E (2023) *Trichoderma*: a multipurpose, plant-beneficial microorganism for eco-sustainable agriculture. Nat Rev Microbiol 21(5):312–326. https://doi.org/10.1038/s41579-022-00819-5
19. Xiang CY, Gao F, Jakovlić I, Lei HP, Hu Y, Zhang H, Zou H, Wang GT, Zhang D (2023) Using phylosuite for molecular phylogeny and tree-based analyses. Imeta 2(1):e87. https://doi.org/10.1002/imt2.87
20. Xie J, Chen Y, Cai G, Cai R, Hu Z, Wang H (2023) Tree visualization by one table (tvbot): a web application for visualizing, modifying and annotating phylogenetic trees. Nucleic Acids Res 51(W1):W587–W592. https://doi.org/10.1093/nar/gkad359
21. Zhang M, Wang R, Khan RAA, Zhan X, Ren S, Jiang H, Zheng C, Wu Y, Yang F, Yu X, Liu T (2025) *Trichoderma asperellum* FJ035 restructure the rhizosphere microbiome to control the cucumber *Fusarium* wilt. Plant Cell Environ 70250. https://doi.org/10.1111/pce.70250
22. Zhang S, Qiu CW, Shi SH, Sreesaeng J, Gao ZF, Zhang C, Mao W, Ali MA, Chen ZH, Wu F (2026) *Trichoderma* genome and multiomics insight into promoting yield and reducing grain cadmium in barley and wheat. J Integr Plant Biol 68(1):39–56. https://doi.org/10.1111/jipb.70063
23. Zhao R, Chen K, Mao L, Zhang C (2025) Eleven new species of *Trichoderma* (*Hypocreaceae*, *Hypocreales*) from China. Mycology-an Int J Fungal Biology 16(1):180–209. https://doi.org/10.1080/21501203.2024.2330400
24. Zhao R, Mao LJ, Zhang CL (2023) Three new species of *Trichoderma* (*Hypocreales*, *Hypocreaceae*) from soils in China. Mycokeys 97:21–40. https://doi.org/10.3897/mycokeys.97.101635
25. Zhuang WY (2020) Flora fungorum sinicorum vol. 60 *Hypocreaceae*. Science, Beijing

Figures

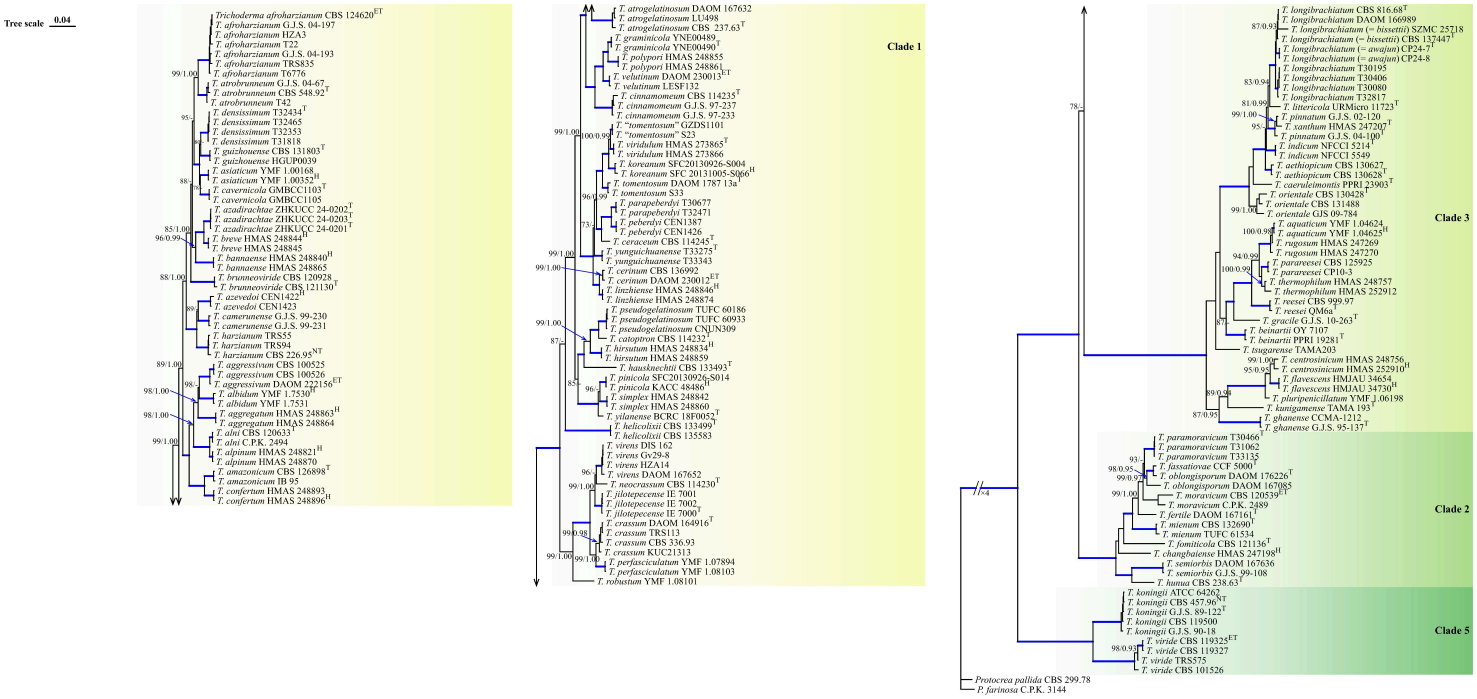


Figure 1

Multilocus phylogenetic tree inferred from concatenated *rpb2* and *tef1* sequences of *Trichoderma*. *Protocrea pallida* and *P. farinosa* are designated as outgroup taxa. Nodal support values are presented as MLBS/BPP; only values MLBS ≥ 70% and BPP ≥ 0.90 are shown, and branches with full support (100% MLBS / 1.00 BPP) are marked in bold blue. Strains newly sequenced in this study are highlighted in red text.

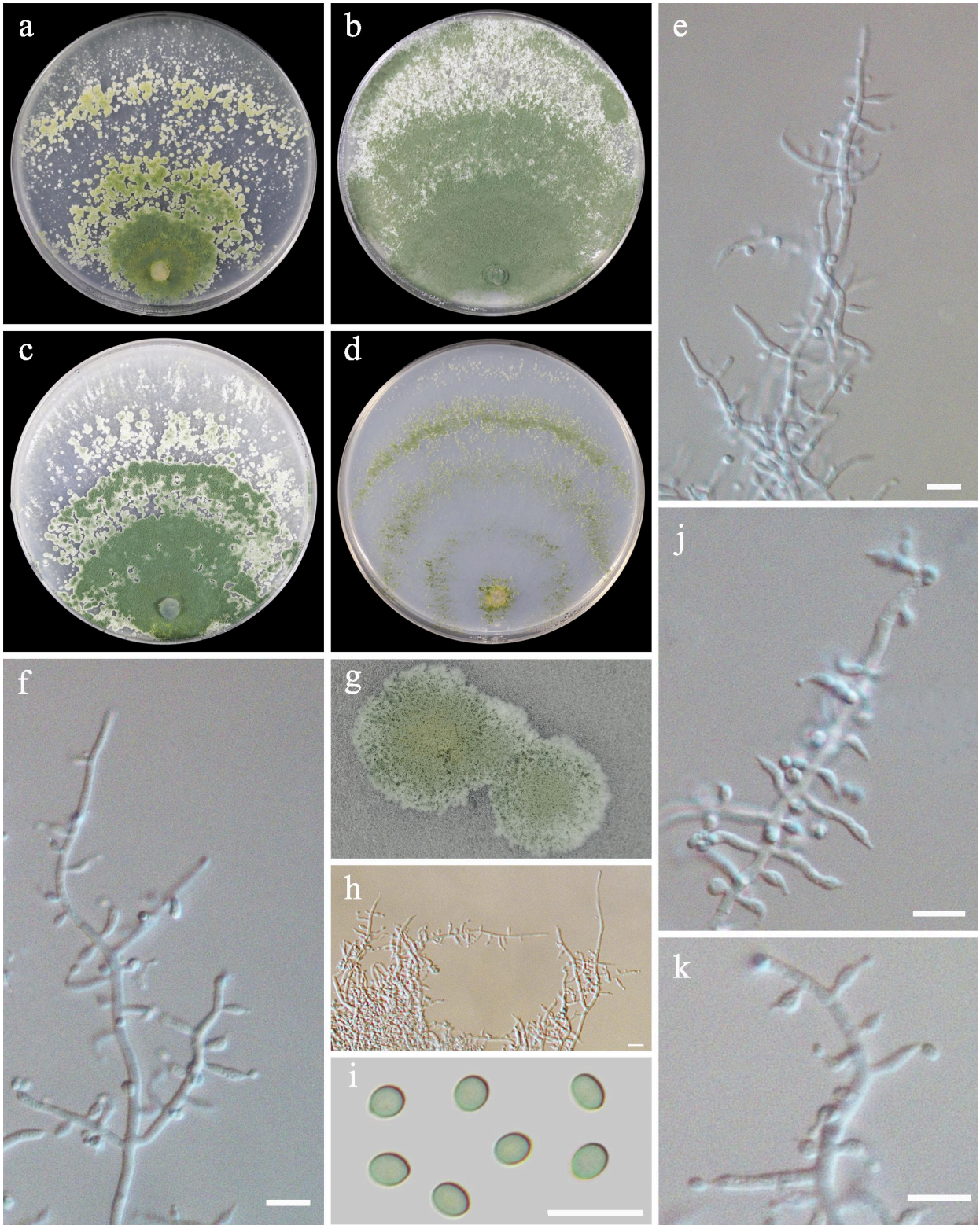


Figure 2

Cultural and micromorphological characters of *Trichoderma longibrachiatum* (isolate T30195). a–d. Seven-day cultures incubated at 25 °C under a 12 h light/12 h dark photoperiod (a. PDA; b. MEA; c. CMD; d. SNA); g. Sporulating pustule on PDA; e–f, h, j–k. Conidiophores and phialides; i. Conidia. Scale bars = 10 μm (e–f, h–k).

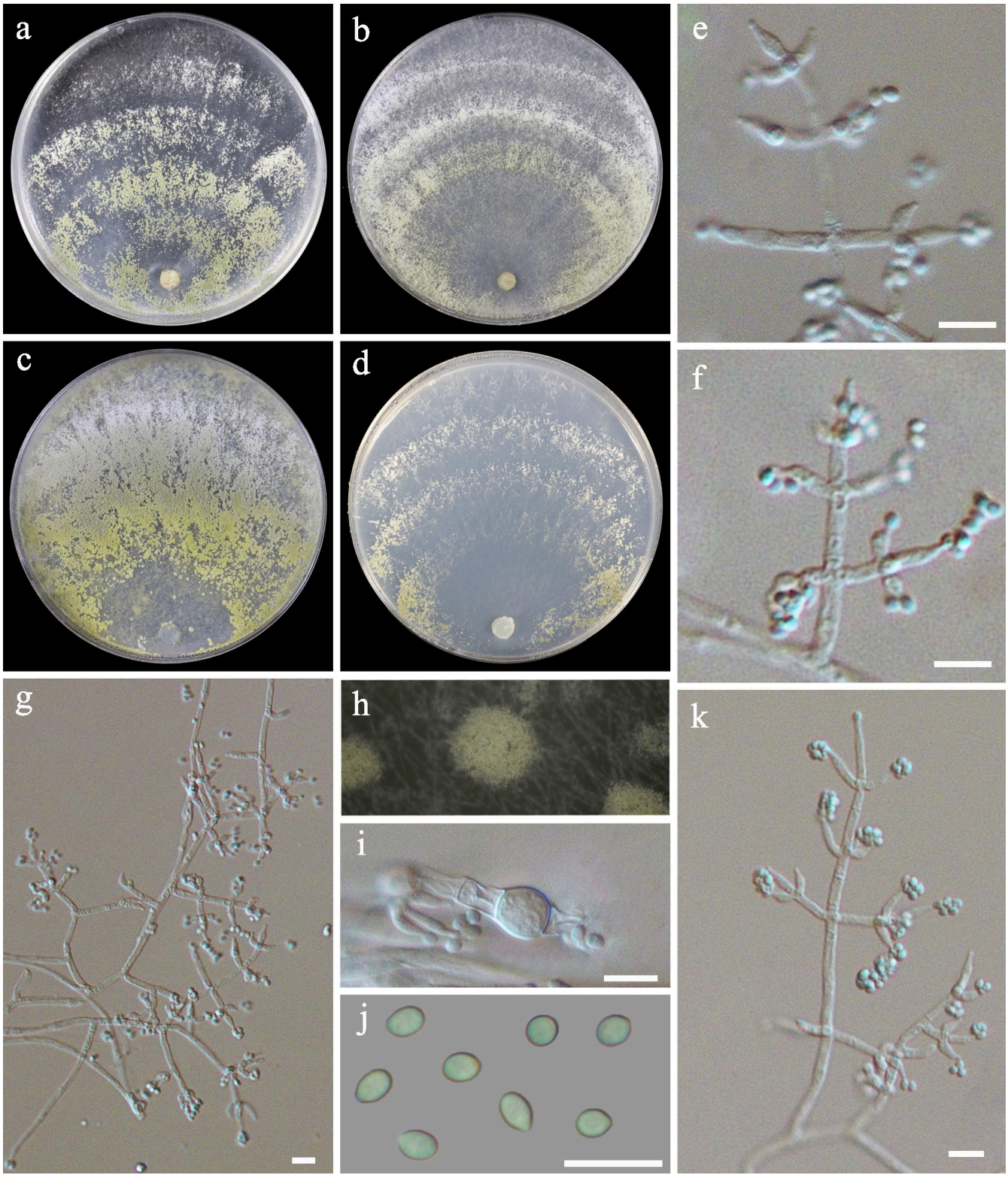


Figure 3

Cultural and micromorphological characters of *Trichoderma paramoravicum* (ex-type T30466). a–d. Seven-day cultures incubated at 25 °C under a 12 h light/12 h dark photoperiod (a. PDA; b. MEA; c. CMD; d. SNA); h. Sporulating pustule on PDA; e–g, k. Conidiophores and phialides; i. Chlamydospores; j. Conidia. Scale bars = 10 μm (e–g, i–k).

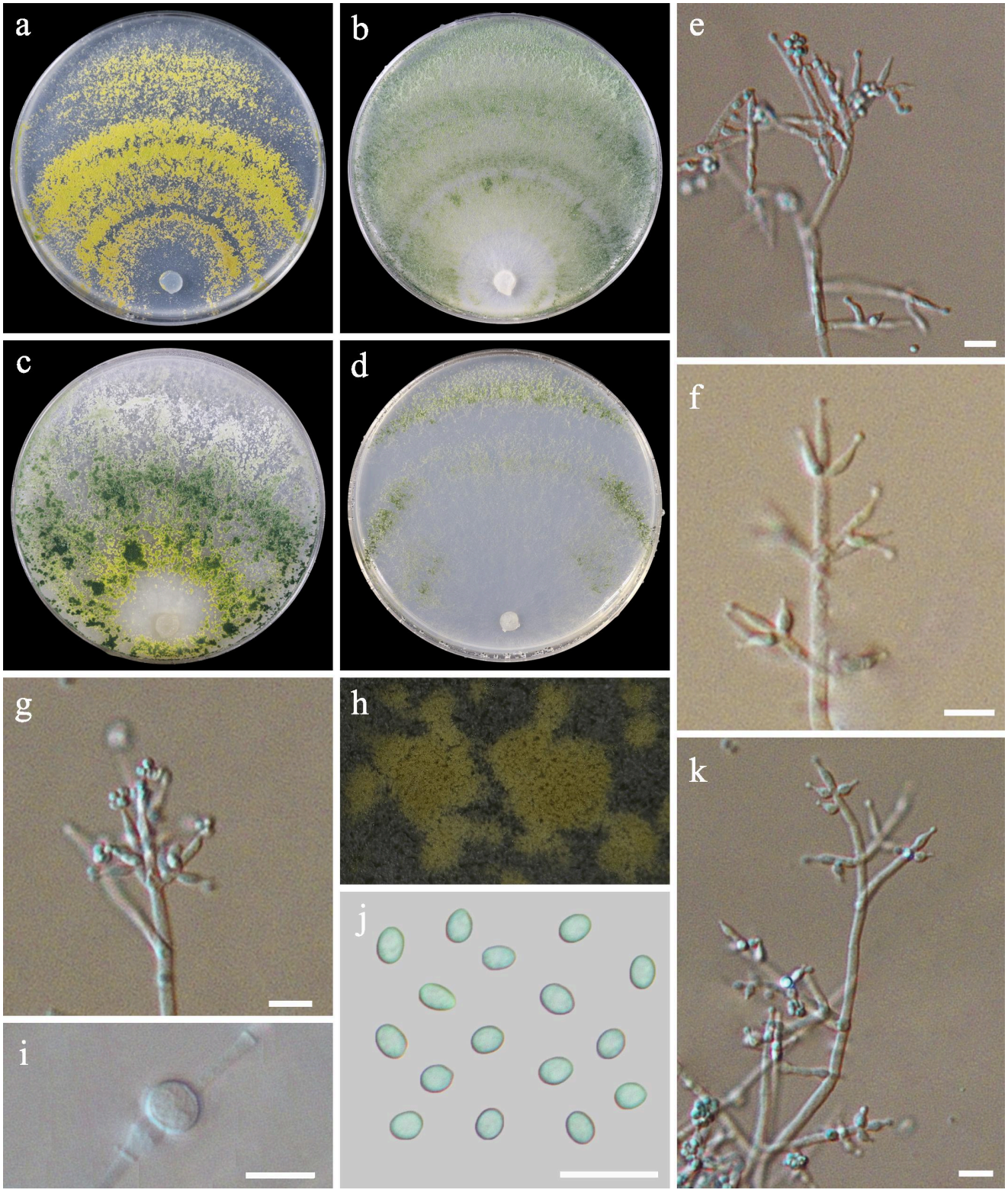


Figure 4

Cultural and micromorphological characters of *Trichoderma yunguichuanense* (ex-type T33275). a–d. Seven-day cultures incubated at 25 °C under a 12 h light/12 h dark photoperiod (a. PDA; b. MEA; c. CMD; d. SNA); h. Sporulating pustule on PDA; e–g, k. Conidiophores and phialides; i. Chlamydospores; j. Conidia. Scale bars = 10 μm (e–g, i–k).